THE JOURNAL OF PHYSICAL CHEMISTRY C

Article

Cite This: J. Phys. Chem. C 2019, 123, 14439−14448

pubs.acs.org/JPCC

Solid-State Nuclear Magnetic Resonance Characterization of Residual ^{23}Na in Aramid Fibers

J. Ole Brauckmann,[†,‡] René Verhoef,[¶] Anton H. M. Schotman,[¶] and Arno P. M. Kentgens*[,‡]

[†]TI-COAST, Science Park 904, 1098 XH Amsterdam, The Netherlands

[‡]Magnetic Resonance Research Center, Institute for Molecules and Materials, Radboud University, Heyendaalseweg 135, 6525 AJ Nijmegen, The Netherlands

[¶]Teijin Aramid B.V., Research and Innovation Center, P.O. Box 5153, 6802 ED Arnhem, The Netherlands

Supporting Information

ABSTRACT: In aramid (*para*-phenylene terephthalamide) fibers, small concentrations of sodium ions are present as remnants of the neutralization step in the production. This is thought to relate to the long-term stability of the fibers. Our study shows that most of the sodium ions are accessible by water. Fitting the ^{23}Na NMR spectra at two magnetic fields reveals a large distribution in both quadrupolar interaction and isotropic chemical shift, indicating substantial structural variations in the direct vicinity of the ions. All these observations imply that, upon drying, the sodium ions reside in a single pool with a very disordered environment. This implies that fibers consist of crystallites that are packed in such a way that end groups are not directly exposed for coordination with sodium. The sodium resides in intercrystalline regions of the fibers, that is, cracks and voids, most likely in the form of sodium sulfate at various stages of (residual) hydration.

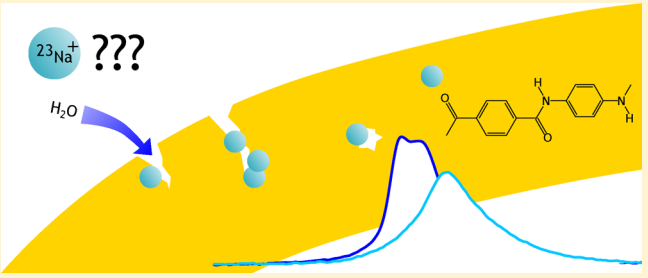

INTRODUCTION

Polyaramid fibers are highly crystalline and have remarkable properties: by their weight, they are stronger than steel, heat-resistant up to 500 °C, and inert to most organic solvents. The high-performance polymer is known to contain some inorganic impurities due to the production process. The highest concentrated impurity is sodium, which remains from the neutralization step in the production. The fibers are spun from anisotropic solutions of 20 wt % *para*-phenylene terephthalamide (PPTA) in sulfuric acid. The acid is neutralized using sodium hydroxide (NaOH). If sulfuric acid is left unneutralized in the aramid fiber, then it would hydrolyze PPTA in the long term. Therefore, it is of interest to know how much sodium is present in the yarn in relation to the amount of acid. Also, the form of sodium in the fiber is of interest as it might reflect the neutralization process and the location of the sodium ions in the fiber. In fact, it is believed that the reaction with remnants of sulfuric acid is one of the main aging mechanisms of the fibers.[1]

In the literature, the presence of sodium in polymers is often interpreted in terms of counterions and ordered salts.[2−4] In this respect, the use of solid-state ^{23}Na NMR for the characterization of such materials is valuable as ordered salts give rise to well-defined powder patterns, which directly reflect the local symmetry around the nucleus and the size of the local electric field gradient, leading to a specific quadrupole interaction.

The series of papers on sulfonated polystyrene (PS) by O'Connell et al. shows how morphological changes, for instance, as a function of humidity, temperature, or molecular weight, are reflected in the ^{23}Na NMR spectra.[5−7] O'Connell et al. observed that, even in a glassy matrix such as polystyrene, all the sodium ions are hydrated.[5]

By comparing the sodium spectra of dried sulfonated PS to model compounds, such as sodium hydroxide and sodium toluenesulfonate, the authors show that ordered salts are not appropriate to describe the sodium in the polymer matrix. The authors conclude that, rather than ordered salts, heterogeneous sodium aggregates are formed, which are characterized by a broad distribution in quadrupolar parameters.[5]

The later papers in the series show how the sodium spectra are influenced by annealing and by the polydispersity of the polymer.[6,7] These reports demonstrate that ^{23}Na NMR provides information about the morphology of the samples and that the remnants of sodium in the samples reflect their processing history.

The remnants of sodium in aramid fibers have been analyzed by single-pulse excitation (SPE) solid-state NMR. Connor and Chadwick compared the ^{23}Na NMR spectra of PPTA to a series of sodium salts to identify the prevalent form in which sodium occurs in the fiber.[8] The authors concluded that sodium is most likely present as sodium carbonate (Na_2CO_3). This is, however, very unlikely as Na_2CO_3 is sometimes used to neutralize sulfuric acid. Since sulfuric acid is the stronger acid,

Received: March 4, 2019
Revised: May 3, 2019
Published: May 7, 2019

DOI: 10.1021/acs.jpcc.9b02071
J. Phys. Chem. C 2019, 123, 14439−14448

Table 1. Sodium and Sulfur Content of the Yarns Used in This Study As Determined by XRF[a]

yarn (% Na)	dtex[b]	# of filaments	S (mmol/kg)	Na (mmol/kg)	predicted Na_2SO_4 (mmol/kg)	predicted COONa (mmol/kg)
1 (0.090%)	1680	2000	38	39[c]	19	0
2 (0.250%)	930	1000	55	109	55	0
3 (0.268%)	1680	1000	38	117	38	41
4 (0.366%)	930	1000	57	160	57	46

[a]The measurement error for sodium and sulfur was determined to be 0.017% (w/w) and 0.006% (w/w), respectively. The last two columns give the expected sodium sulfate and sodium terephthalate concentrations. [b]Mass of the yarn in grams per 10.000 m. [c]Neutralized with sodium carbonate instead of sodium hydroxide.

the formation of sodium sulfate is more likely. Furthermore Na_2CO_3 is known to give a well-defined NMR powder pattern, which was not observed in the ^{23}Na spectrum of PPTA.[8]

To our knowledge, sodium in aramid fibers has, since this early report, not been characterized using modern high-field solid-state NMR. A challenge in the analysis of the residual sodium in aramid fibers is the very low concentration. Typically, only 0.1−0.3 wt % sodium remains in the fiber.[1,9,10] Although sodium is 100% abundant, it is still challenging to study such low concentrations by NMR particularly when broad lines are encountered due to the quadrupolar interaction. The availability of high external magnetic fields (B_0) helps in this regard as the second-order quadrupolar interaction scales with $\propto \frac{1}{B_0}$. At higher fields, the quadrupolar linewidth reduces in addition to the favorable Boltzmann polarization factor, which enhances the feasibility of studying low sodium concentrations.

In the spectra by Connor and Chadwick,[8] asymmetrically broadened line shapes are observed, which suggest that the resonances of the sodium ions in aramid fibers are best described by a distribution in quadrupolar parameters. Distributions in quadrupolar interaction parameters have been observed in glasses and otherwise disordered materials. Local disorder gives rise to a variation in bond angles and distances to neighboring nuclei. This disorder is reflected in a variation in chemical shift and electric field gradient (EFG) and its asymmetry parameter η_Q.

Quantification of the EFG distributions in relation to structural disorder is possible using the model by Czjzek et al.,[11] which provides a probability distribution for the principal component V_{zz} of the EFG tensor and its asymmetry parameter η_Q in relation to the disorder, which is postulated to result in normal distributions of the five independent elements defining the (traceless) EFG tensor. The validity of this model has since been studied in detail, and an implementation for the description of NMR spectra has been defined.[12−14] In the context of NMR experiments, it was realized that this model is too limited to describe systems with a fairly well-defined local coordination and disorder in the higher coordination spheres, calling for an extension that should warrant the isotropic nature of the disorder and the fact that the EFG tensor elements remain normally distributed.[15,16] In MAS NMR, spectra of half-integer quadrupolar nuclei subject to local disorder, asymmetrically broadened line shapes are observed, which tail to the high-field (low-ppm) side. Such line shapes can be described using the aforementioned models to estimate the average quadrupolar coupling constant and its distribution. In addition, one can extract information about the width of the isotropic chemical shift distribution when spectra are acquired at different magnetic field strengths since the quadrupolar and chemical shift interactions have different field dependencies ($\sim 1/B_0$ and $\sim B_0$, respectively).

In this study, we analyze the sodium spectra of aramid fibers as a function of sodium concentration and hydration. We report quantitative single-pulse excitation (SPE) spectra at different external fields and a multiple-quantum magic-angle spinning (MQMAS) experiment to estimate the variation of the quadrupolar and chemical shift interactions of sodium ions present in aramid fibers. Finally, we discuss the implications of our results for the morphology model of the polymer fiber.

WATER AND SODIUM IN ARAMID FIBERS

Based on the X-ray structure, the density of PPTA is expected to be around 1.5 g/cm^3. The density of aramid fibers is, however, in the range of 1.43−1.45 g/cm^3.[17] The discrepancy with the X-ray structure is explained by the presence of cracks and voids in the structure, which often hold water.[8,18,19]

The unit cell of PPTA leaves no space for the presence of water between the hydrogen-bonded polymer chains, and therefore, the uptake of water by aramid polymers has been linked previously to the presence of sodium ions, for example, in the form of sodium sulfate.[18] Elemental analysis proves that, among other impurities, 0.1−0.3 wt % sodium is present in the fiber.[1,19] Interestingly, an X-ray study reports the presence of ordered sodium salts such as sodium sulfate/sulfite or sodium carbonate.[20] The author also mentions that the presence of ordered sodium salts was rather exceptional and should thus be interpreted as an impurity.

Chadwick and Connor calculated that, if all the water, up to 6 wt %, would reside on the skin of the fiber, it would be 600-monolayers-thick.[8] By the weak interaction, this layer would not remain around the fiber, and therefore, large fractions of the water must be located in the interior of the fiber.

More recent studies show that, in addition to cracks, two distributions of micro- and macrovoids are present in aramid fibers.[21,22] It is a long-standing question whether these voids are related to clustering of specific chemical groups. Morgan et al. speculated on the clustering of end groups in such voids as well as on clustering of sodium to compensate the charge of the polar groups.[1] To our knowledge, the location of the end groups in the fiber has not been elucidated yet as no analytical technique is available to probe the chemical nature in combination with spatial resolution.

When chemical specificity and quantification are desired, usually NMR is the method of choice. Unfortunately, the end-group concentration is low since the chain length is expected to be on the order of 100 repeat units and the natural abundance of the ^{13}C or ^{15}N nuclei is very low (1.1 and 0.37%, respectively). The combination of low concentration and low abundance therefore poses a challenge for the quantification of the end groups by NMR.

DOI: 10.1021/acs.jpcc.9b02071
J. Phys. Chem. C 2019, 123, 14439−14448

MATERIALS AND METHODS

Samples. In this study, four different Twaron aramid yarns with a sodium content ranging from 0.09 to 0.366 wt % were supplied by Teijin Aramid BV (Table 1). The sodium and sulfur content was determined by X-ray fluorescence (XRF).

The degree of neutralization and thus the sodium content vary between the yarns. Beside residual sulfuric acid, the yarns also contain carboxylic end groups. The exact carboxylic end-group concentration is unknown, but it is known that the chain length is approximately 100 repeat units. This corresponds to about 100 mmol of end groups (amino and carboxyl) per kg. As it is assumed that there are more carboxylic acid end groups than amine groups, there are at least 50 mmol of carboxylic acid end groups per kg. When we assume that the sulfuric acid, being the stronger acid, is neutralized before the carboxylic end groups, a prediction toward the identity of the sodium species in the yarns can be made. It is summarized in Table 1. The first yarn was neutralized with sodium carbonate and the last three yarns with sodium hydroxide. The samples were thoroughly dried for at least 24 h in an oven at 120 °C before ^{23}Na NMR measurements.

Solid-State NMR. Quantitative single-pulse excitation (SPE) spectra were recorded using a VNMRS 9.4 T and a VNMRS 20.0 T NMR spectrometer employing 80 kHz rf field strength and excitation pulses of $<\frac{\pi}{6}$ to warrant quantitative excitation.[23,24] The SPE spectra were processed without baseline correction and integrated including the spectral region of the first-order sidebands of the center transition. Further acquisition parameters are given in the caption of the figures.

MQMAS experiments were recorded at 20.0 T external field using a 1.6 mm MAS probe head since better efficiencies are obtained using higher rf fields for 3Q excitation and reconversion. The pulse lengths were 3.9 and 1.3 μs for excitation and reconversion, respectively, at an rf field of approximately 180 kHz. The parameters were optimized on Na_2SO_4 since the low concentrations in the samples did not allow for a quick parameter optimization. For all the measurements, we verified that the rotors were background-free and that the recycle delays were long enough to ensure full relaxation of the spins. Chemical shifts are reported relative to an aqueous solution of NaCl (0.1 M) referenced to 0 ppm.

RESULTS

Quantitative SPE Spectra. To investigate the sodium content of the fibers, we recorded quantitative single-pulse excitation spectra. The spectra recorded, accumulating 32,000 averages each, are shown in Figure 1. More averages were recorded for the 0.09 wt % sample, and its intensity was scaled accordingly.

Since the NMR experiments are, in principle, quantitative as we use short pulses and fast MAS,[24] we derive the sodium content from the integral of the spectra. In Table 2, the sodium content determined by NMR is compared to the sodium content by XRF. In principle, the absolute sodium content can be determined by comparing the integrated intensity to an external standard such as sodium chloride or sodium sulfate. Here, we choose to use integrals for relative comparison only using the integral of the sample with the highest sodium concentration, as determined by XRF, as a reference. The relative intensities derived from the SPE measurements are in good agreement with the values determined from XRF and show that the spectra can be interpreted quantitatively.

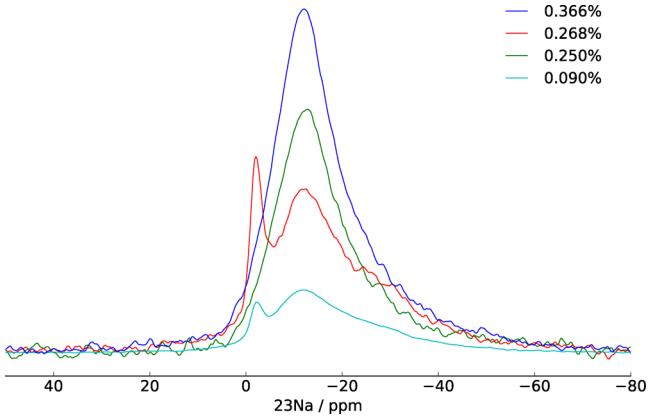

Figure 1. Quantitative SPE spectra of all the samples recorded by accumulating 32,000 averages with a recycle delay of 0.5 s at an external field of 9.4 T and a spinning speed of 10 kHz. For the 0.090% sample, more averages were required for good signal to noise (1,536,000 averages with a recycle delay of 20 ms). The intensity is scaled by the number of scans and the weight of the rotor. No signs of the satellite transitions are visible in the spectra due their large linewidth, inefficient excitation, and possibly dynamics.

Table 2. Sodium Content Determined by X-ray Fluorescence (XRF) and Derived by Solid-State SPE ^{23}Na NMR (SPE NMR)

XRF	SPE NMR[a]
0.366 ± 0.017[b]	0.366 ± 0.03[c]
0.250 ± 0.017	0.247 ± 0.03
0.268 ± 0.017	0.236 ± 0.03
0.090 ± 0.017	0.094 ± 0.01

[a]Integral of highest concentrated samples was set to 0.366%. [b]The error is estimated from repetitive measurements (n = 5) and is 0.017% (m/m). [c]The error is estimated from repetitive analyses and takes into account possible phase misadjustments for the broad resonances. The error is smaller for the 0.090 sample because of the better SNR of the spectrum of this sample (larger amount of averages acquired).

For all samples, we observe a broad asymmetric featureless line, also for the yarns (3 and 4) where one could expect a second sodium species based on the sulfur/sodium stoichiometry. In addition to the broad component, we observe a small narrow line around −2 ppm for the 0.090% and the 0.268% sample (yarns 1 and 3, respectively).

The broad component is attributed to sodium in the polymer fiber. The fact that no clear quadrupolar pattern is observed for these samples proves that the sodium ions are not in a well-defined crystalline environment as in an ordered salt but experience a variation in local coordinations so that the spectra are best described by a distribution in quadrupolar parameters. In fact, the appearance of the spectra is very similar in term of chemical shifts and linewidths to the spectra reported by O'Connell et al. for sodium ions in sulfonated polystyrene.[5]

Narrow lines for quadrupolar nuclei are only observed for symmetric environments such as cubic salts or for solutions where the quadrupolar interaction is averaged by the isotropic motions. Turoscy et al. reported that many cubic salts of sodium resonate around 7.4 ppm.[25] By the chemical shift, it is thus more likely that the narrow resonance in the 0.268 and 0.090 wt % spectra is due to hydrated sodium ions that remain trapped in voids of the fiber despite thorough drying. As these

DOI: 10.1021/acs.jpcc.9b02071
J. Phys. Chem. C 2019, 123, 14439−14448

are the thicker yarns (compare Table 1), it seems plausible that small amounts of water remain trapped in these fibers.

In the systematic study of sulfonated polystyrene, also a narrow resonance in this region (−2.7 ppm) is observed for dried samples.[7] The authors of this study attribute this line to a change in morphology as it is only observed for monodisperse samples.

Furthermore, the study by Wang and Ando shows that the chemical shift of sodium depends on the concentration.[26] Therefore, the shift below 0 ppm could be a concentration effect. This would hint to small pore sizes, which are only filled with a few equivalents of water and are not accessible from the outside. It has been estimated by Mauritz and Moore that, for sodium, approximately four to six water molecules per ion are enough to obtain an isotropic resonance line close to 0 ppm.[2,27]

We note that the spectra of the 0.09 and 0.268 wt % samples, as well as the 0.366 and 0.250 wt % samples, are very similar. As these yarns are made up of the same number of filaments, the additional resonance could reflect the morphology of the different yarns.

Effects of Hydration. For most applications of the fiber, the hydrated state of the fiber is the most representative form. Rehydration experiments by Chadwick and Connor show that most of the water, up to 6 wt %, is absorbed within 24 h, but even after 5 days, the weight still increases.[8]

In the NMR probe, the opposite experiment—in situ drying of the aramid fiber—is easier to implement. We use the fact that the top cap of the ZrO_2 rotor has a small hole, and thus, water vapor can enter into or escape from the rotor. To establish equilibrium humidity, we stored the rotor for more than a week in 100% relative humidity.

The dehydration takes place during NMR experiments by the dry N_2 atmosphere that is used for the spinning of the rotor. By the rotation, weakly adsorbed water will quickly escape from the rotor. More strongly interacting/absorbed water will slowly diffuse through the hole in the cap out of the rotor.

In Figure 2, the ^{23}Na SPE spectra are shown as a function of dehydration time. Every spectrum is recorded, adding 15,000 scans (7.5 min). The changes in the spectrum reflect the changes of the hydration state of the sodium ions in the fiber.

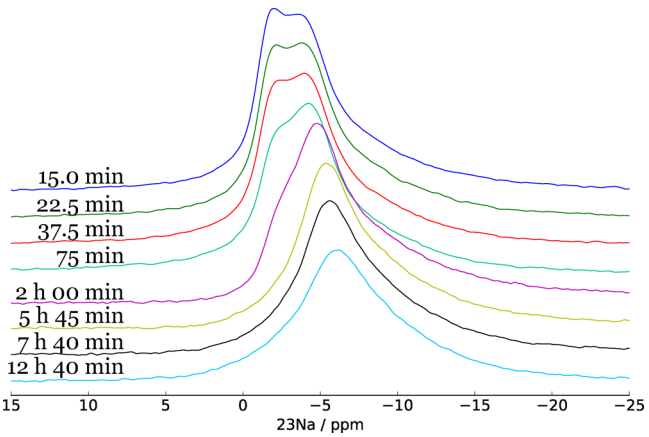

Figure 2. In situ drying of the 0.250 wt % fiber inside the 20.0 T NMR spectrometer followed by ^{23}Na SPE spectra. Each spectrum is recorded, adding 15,000 averages in a 4 mm ZrO_2 rotor at 10 kHz MAS at 25 °C. The time of drying is indicated for the individual spectra.

In the first spectrum (15 min), clearly two components with their maxima at −2 and −4 ppm are recognized. The line at −4 ppm tails to the low ppm side, which could hint to a third broad component or an exchange-broadened resonance (due to exchange of water over clusters at an intermediate state of hydration). Since we observe changing of the relative intensities of the two resonances, an exchange-broadened second component appears more likely. This is, for instance, visible in the spectrum after 2 h, where the resonance around −2 ppm is strongly reduced and that around −4 ppm moved to lower ppm values and became broader. The narrow line at approximately −2 ppm has also been observed in the quantitative SPE spectra above (Figure 1) and was attributed to solvated sodium ions.

Earlier studies suggest that the chemical shift of aqueous solutions of alkali metal halides is concentration-dependent. This has been shown by Turoscy et al. for the chemical shift of cesium chloride solutions.[28] The ^{7}Li chemical shift, however, is independent on the concentration. The study by Wang and Ando on sodium and its hydration as a function of water content in poly(aspartic acid) sodium/poly(vinyl alcohol) blends suggests that the chemical shift of sodium does depend on the concentration.[26] It should be noted that the study by Wang and Ando was carried out on a 300 MHz machine and, therefore, the resonance will not only start to shift by the increased concentration but also by the quadrupolar-induced shift (q_{IS}) due to the second-order quadrupolar interaction as soon as sodium starts to aggregate. The q_{IS} is proportional to the strength of the quadrupolar interaction. During the drying process, the q_{IS} will increase by aggregation of the sodium ions from the solution.

This effect explains the observation in Figure 2; upon drying, first, the narrow line at −2 ppm is depleted. At the same time, the line at about −4 ppm increases and then starts to shift toward lower ppm values by the increasing q_{IS}. Throughout this series of experiments, the relative intensity of the broad component increases since the sodium ions cluster upon dehydration. The low ppm resonance broadens and its center of gravity—the point where the integrated parts to the left and to the right are equal—moves to lower ppm values by the increasing quadrupolar interaction. We interpret this as the shifting of equilibrium of the exchanging sodium ions toward the aggregated form.

The observation that, initially, most of the sodium ions are hydrated suggests that the crack and void structure is very open as most of the sodium ions can be reached by water. Similar observations have been made by O'Connell for PS but also earlier by Chadwick and Connor for aramid fibers.[5,8] The broadening of the line is attributed to the aggregation of sodium ions in the fiber: the environment of the sodium ions changes due to association with the polar groups of the polymer or counterions. Without water, it is more difficult for the sodium atoms to have a symmetric coordination, and therefore, the quadrupolar interaction increases upon dehydration. We verified that the spectrum recorded after 12 h coincides with that of the dry 0.250 wt % sample. It is typified by one broad asymmetric component.

NMR Characterization of Sodium in Aramid. The SPE spectra of the in situ drying (Figure 2) suggest that, by the appearance of the broad asymmetric line shape, the sodium ions in the fiber are best described by a distribution in

DOI: 10.1021/acs.jpcc.9b02071
J. Phys. Chem. C 2019, 123, 14439−14448

quadrupolar and, possibly, chemical shift parameters, which is investigated in more detail by field-dependent SPE and MQMAS experiments.

Field Dependence. As the field dependence of the chemical shift and quadrupolar interaction is opposite, this can be used to separate their contributions to the linewidth. The chemical shift interaction (in Hz) scales linearly with the external magnetic field, whereas the second-order quadrupolar interaction scales with the inverse of the external magnetic field.

In Figure 3, the SPE spectra acquired at external field values of 9.4 and 20.0 T are compared. Both spectra are acquired using 10 kHz MAS and are processed in the same way using 100 Hz exponential line broadening. At a lower field, the maximum of the spectrum shifts upfield (lower ppm) and broadens significantly. This is indicative of a sizeable quadrupolar interaction.

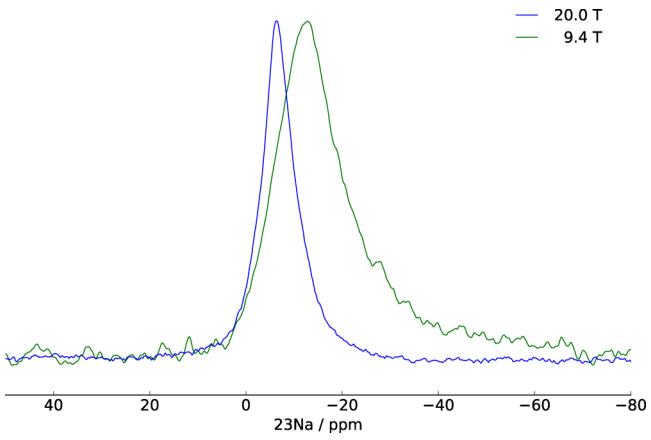

Figure 3. Comparison of the ^{23}Na SPE spectra of the 0.250 wt % recorded at two different external magnetic fields. The spectra are scaled to the same intensity to ease the comparison.

For a second-order quadrupolar interaction, the center of gravity (δ_{F2}) of the powder pattern does not coincide with the isotropic chemical shift (δ_{iso}).[24] It is shifted by the quadrupolar-induced shift q_{IS}, which is field-dependent, as explained in detail in the Supporting Information. For a resonance that is dominated by a distribution in quadrupolar parameters, C_Q and η_Q can no longer be determined independently, but the quadrupolar interaction product $P_Q = C_Q\sqrt{\left(1 + \frac{\eta_Q^2}{3}\right)}$ enters the expression for the quadrupolar-induced shift (see the Supporting Information).

It is impossible to extract the contribution of a chemical shift distribution from a single spectrum as both the quadrupolar and chemical shift distributions lead to broadening of the resonance. We observe that the spectrum recorded at a lower field (green trace, Figure 3) is much broader in terms of ppm and shifts to lower ppm due to a larger q_{IS}, so we conclude that the quadrupolar interaction is a major contribution to the linewidth, particularly at 9.4 T.

Assuming that the distribution in isotropic chemical shift and the second-order quadrupolar interaction are the dominant interactions contributing to the linewidth (i.e., field-independent dipolar interactions are considered negligible), the contribution of these interaction can be estimated from the full width at half maximum (FWHM) in Hz. Interestingly, this FWHM is almost identical at both fields: 1550 Hz at 9.4 T and 1600 Hz at 20 T. Based on their field dependence, we can therefore get estimates for the contributions to the linewidth of the isotropic chemical shift distribution (Δ_{CSD}) and the second-order quadrupole interaction (Δ_Q) by solving the following equations

$$\mathrm{FWHM}(9.4\ \mathrm{T}) = \Delta_{CSD} + \Delta_Q = 1550\ \mathrm{Hz} \quad (1)$$

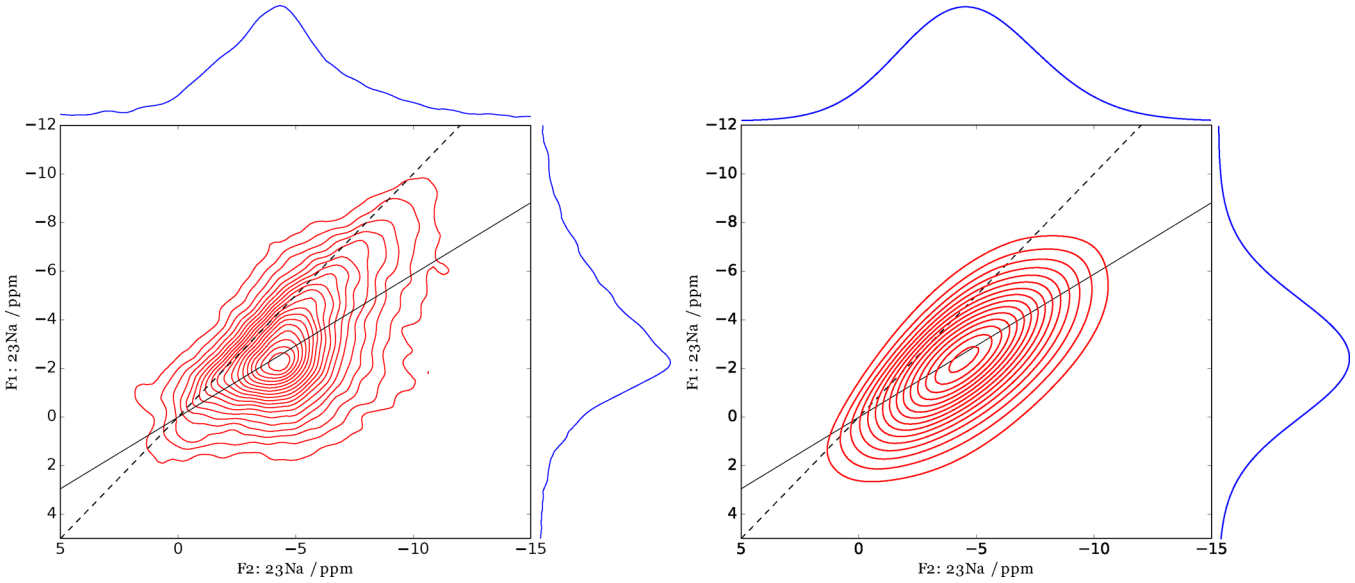

Figure 4. Left: 3Q-MQMAS spectrum of the 0.250 wt % sample. The spectrum was acquired using 15 kHz MAS and 30,360 averages with 0.12 s recycle delay at 20.0 T. Thirty complex points were recorded ($t_{1,max}$ = 960 μs). During 3Q evolution, high-power SPINAL64 proton decoupling was used. The spectrum is sheared, and the indirect dimension is scaled by 9/34. Exponential line broadening (100 Hz) was applied in the direct dimension. Twenty linear contours from 10 to 100% are shown. Right: Fitted MQMAS spectrum assuming an extended Czjzek model carried out using the ssNake software (ref 31). The parameters are described in the main text.

DOI: 10.1021/acs.jpcc.9b02071
J. Phys. Chem. C 2019, 123, 14439−14448

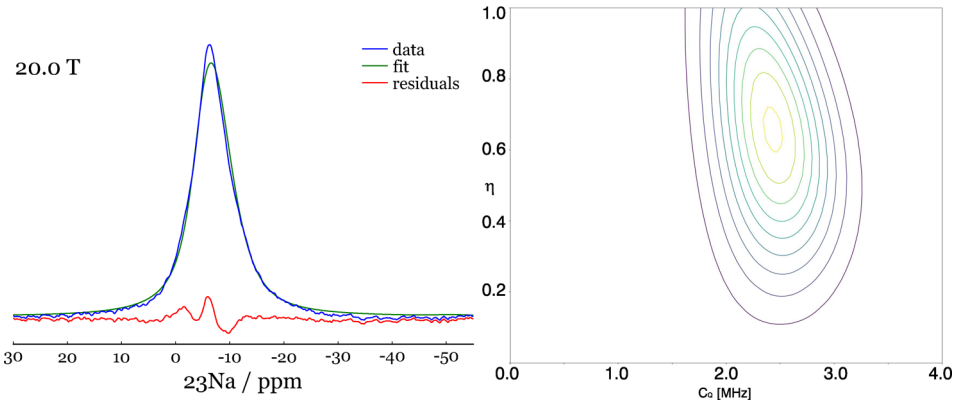

Figure 5. Left: SPE spectrum of the 0.250 wt % sample acquired at 20.0 T field. For the fit, an extended Czjzek model was assumed with $\delta_{iso} = -3.5$ ppm, σ_{CS} = 1150 Hz (5 ppm), and local quadrupolar parameters of $C_{Q,0}$ = 2.3 MHz and η_0 = 0.64 and a σ_Q of 0.4 MHz. Right: Probability distribution for the C_Q and η_Q arising from the extended Czjzek model.

$$\text{FWHM}(20.0\text{ T}) = \frac{20.0}{9.4} \times \Delta_{CSD} + \frac{9.4}{20.0} \times \Delta_Q = 1600\text{ Hz} \quad (2)$$

This results in a contribution of the isotropic chemical shift distribution to the linewidth at 9.4 T of about 520 Hz (5 ppm) and a contribution of the quadrupole interaction of 1030 Hz. At 20 T, the relative contributions of these terms are reversed, that is, 1100 Hz (5 ppm) for the distribution in the chemical shift and 500 Hz for the quadrupolar contribution.

MQMAS. MQMAS experiments can be used to separate the anisotropic and isotropic parts of the quadrupole interaction in two dimensions.[29,30] The spectra obtained after a shearing transformation hold the anisotropic powder patterns in the direct dimension (F2), while the position in the indirect dimension (F1) reflects the isotropic chemical shift and quadrupolar-induced shift. Due to the lower sensitivity related to the triple-quantum excitation and reconversion, the experiment is challenging in the view of the low sodium concentrations in the present study. An MQMAS experiment has the advantage that it can reveal the presence of chemically different sites, which overlap in the 1D spectra. Furthermore, lines subject to distributions in quadrupolar interaction and chemical shift show characteristic line shapes that lay in distinct directions in the two-dimensional plane.[24]

In the left panel of Figure 4, the triple-quantum (3Q)-filtered MQMAS spectrum acquired at 20 T for the dry 0.250 wt % sample is displayed. This spectrum does not show any obvious sign of different sodium sites but suggests a single resonance subject to a sizeable distribution in both isotropic chemical shift and quadrupolar interaction.

The dashed diagonal in the panel of Figure 4 indicates the isotropic chemical shift line, where resonances that are not affected by a quadrupole coupling would resonate. The large broadening of the spectrum along this direction is indicative of a distribution in isotropic chemical shift, which can be estimated to be of the order of 5 ppm. The solid black line indicates the slope of the quadrupolar-induced shift. As discussed above, the q_{IS} shifts the center of gravity to lower ppm values. Following the convention for scaling and referencing described by Engelhardt et al.,[32] it is possible to get a first estimate for the average quadrupolar interaction product P_Q from the position of the center of gravity of the line in the direct and indirect dimensions, resulting in a P_Q of approximately 1.8 MHz.

Thus, the MQMAS spectrum confirms that sodium is not present as an ordered salt but in a state with significant local disorder that may be characterized by an (extended) Czjzek distribution and a distribution in chemical shift, as already suggested by the analysis of the 1D spectra at different fields. The parameters extracted from these linewidths and the position and pattern of the 2D data show good agreement, confirming a substantial distribution in isotropic chemical shift and a sizeable average quadrupolar interaction of the order of 2 MHz. More detailed insights must come from fitting/simulation of the data based on the (extended) Czjzek model.

Czjzek-Model Fitting. To get a more detailed insight into the NMR parameters of ^{23}Na in the aramid fiber, we decided to fit the NMR spectra using either regular or extended Czjzek distributions using the ssNake package.[31] Fitting the MQMAS spectrum with a regular Czjzek distribution does not give a satisfactory result; both the overall line shape and peak maximum do not correspond well to the experimental spectrum. Better results are obtained using the extended Czjzek model, as displayed in the right panel of Figure 4. This results in an (average) isotropic chemical shift of −1.6 ppm with a distribution of 1150 Hz (5 ppm). The fixed quadrupolar contribution of the local coordination is $C_{Q,0}$ = 2.3 MHz and $\eta_{Q,0}$ = 0.65, whereas the disorder is characterized by a distribution parameter σ_Q = 0.3 MHz (following the convention of Le Caer et al.[15]). It should be noted that extracting the quadrupolar distribution parameters from a single MQMAS spectrum is hampered by the fact that the 3Q excitation and reconversion depend on the ratio of the quadrupolar coupling strength and radio-frequency field strength. As a result, sites experiencing large quadrupolar interactions are attenuated in the MQMAS spectrum. Nevertheless, the parameters are good starting values for a detailed fit of the field-dependent SPE spectra. It proved impossible, however, to get a consistent fit of these spectra using the same parameter set. This is attributed to experimental shortcomings for the spectrum acquired at 9.4 T. Here, the limited spinning speed truncates the width of the quadrupolar distribution. Sato et al.[33] observed that the linewidth of quadrupolar nuclei in glasses increases with increasing spinning speeds up to a certain point. At lower spinning speeds, sites with a large C_Q only contribute weakly to the central transition resonance because their centerband and sidebands are not well separated.[24] This means that only the spectrum obtained at 20 T can be expected to give a credible representation of the

DOI: 10.1021/acs.jpcc.9b02071
J. Phys. Chem. C 2019, 123, 14439−14448

quadrupolar distribution. This is corroborated by the fact that all spectra can be simulated using the same $C_{Q,0}$ and $\eta_{Q,0}$ for the extended Czjzek distribution, but the distribution parameter σ_Q increases, going from the MQMAS spectrum to the 9.4 T spectrum. By fixing the chemical shift distribution to 1150 Hz (5 ppm) in the fitting of the 20 T spectra, an average chemical shift δ_{iso} of −3 ppm is obtained, whereas the fixed quadrupolar contribution in the extended Czjzek model is $C_{Q,0}$ = 2.3 MHz and $\eta_{Q,0}$ = 0.64. The disorder in quadrupolar parameters is characterized by a σ_Q of 0.4 MHz (Figure 5). The probability distribution for the quadrupolar coupling constant C_Q and the asymmetry parameter η_Q for these values are represented in the right panel of Figure 5.

Again, the fit of the line shape is not perfect; this is attributed to the limitations of the extended Czjzek model. This model assumes an ordered local coordination of the nuclei with disorder coming from variations in higher coordination spheres. It is more likely, however, that there is also disorder in the local coordination without being completely random, as assumed in the Czjzek model. Nevertheless, although not perfect, the fits of the spectra show that the sodium ions in the fiber can be characterized by a single distribution in NMR parameters for all the spectra acquired at 20 T field. Actually, we tried fitting with a two-site model, but this did not lead to consistent fits for all three spectra. An additional MQMAS experiment performed at 14.1 T and higher MAS speed (shown in Figure S2) confirmed the presence of a single (hydration-sensitive) resonance for yarn 3. All NMR experiments suggest that the sodium ions in the fiber occur in the form of very disordered aggregates that give rise to a large variation in both chemical shift and quadrupolar interaction.

To get better insight into the state of the sodium ions, we look at the quadrupolar parameters of sodium salts that could be present based on the neutralization process. The following ion pairs are conceivable: sodium sulfate (derived from sulfuric acid); sodium benzoate, sodium carbonate, or sodium bicarbonate (derived from terephthalic acid moieties). Since sodium hydroxide is used in the neutralization, sodium hydroxide could also remain in the fiber. All these salts are known to give well-defined quadrupolar powder patterns. The quadrupolar parameters from literature are summarized in Table 3. For some of the salts, multiple sodium sites exist by the symmetry of the packing in the unit cell. For these, multiple rows give the parameters of the different sites.

Based on the 1D and 2D NMR experiments, it is clear that none of the crystalline salts in the table occurs as such in the aramid fibers. O'Connell et al. observed amorphous NaOH at very high sodium concentrations. However, this form resonates at much higher chemical shift, and therefore, amorphous sodium hydroxide can be excluded as a possibility for the state of the sodium ions in the fiber.[5] The question to be answered for further insights into the state of sodium ions is how the quadrupole parameter of disordered quadrupolar nuclei compare to ordered ion pairs such as the salts in Table 3. Our observations clearly indicate that none of the well-defined salts in Table 3 is present in the fiber, but amorphous sodium aggregates form. It is interesting to note, however, that the average found in our distribution of quadrupolar NMR parameters is rather close to the NMR parameters found for Na_2SO_4.

Table 3. Quadrupolar Parameters of Relevant Sodium Salts

compound	δ_{iso} (ppm)	C_Q (MHz)	η_Q	reference
derived from sulfuric acid				
Na_2SO_4	0	2.64	0.62	8
derived from carboxylic acid				
$NaC_7H_5O_2$		0.372	0.75	34
Na_2CO_3	8	1.2	0	8
	3	2.5	0.4	
$NaHCO_3$	−6.25	[a]	[a]	8
derived from sodium hydroxide				
NaOH	21	3.5	0	35

[a]Not specified in ref 8.

DISCUSSION

At ambient conditions, a very large fraction of the sodium ions in polymer systems are hydrated. Therefore, the ion pairing or ordered salts discussed in the literature for polymer systems is at least misleading as the ions will be moving around in a hydrated state. For the system, we study here the sodium diffused into the yarn in the neutralization step. We observe that most of the sodium in the aramid fibers is accessible by water. This suggests that the sodium ions can also diffuse through the fiber. The reports on sodium in different polymers suggest that sodium tends to hydrate easily in all the polymer systems and is directly related to the water uptake of many polymers.

The 1D SPE spectra of dried samples show that the sodium ions are in a disordered environment with an average coupling strength similar to the quadrupole interaction observed for some well-defined sodium salts. Interestingly, similar spectra are obtained at all sodium concentrations. The only difference in the spectra, the additional narrow component for the 0.090 and the 0.268% yarn, is most probably related to the thickness of the fibers. From our results, one cannot determine which counterparts the sodium ions coordinate based on the size of the quadrupole interaction alone. From the literature, it is known that most of the sodium ions are present in the form of sodium sulfate.[1,10,18] Therefore and by the fact that the sodium was introduced to neutralize sulfuric acid, sodium sulfate is the most probable form. Since crystalline sodium sulfate gives a well-defined quadrupolar powder pattern, sodium in the polymer is most likely present in disordered aggregates of sodium sulfate, possibly with some residual H_2O molecules present.

For sulfonated PS and Nafion, sodium is believed to form heterogeneous aggregates that cluster in ion-rich domains, which, by the heterogeneity in the cluster size and by interactions with surrounding ions, also give rise to a variation in quadrupolar parameters.[5,27] Since the appearance of the sodium spectra in the aramid fibers is very similar to the spectra observed for sulfonated PS and Nafion, it is likely that such ion-rich domains are also present in the aramid fibers.

Morgan et al. speculated about the presence of ion-rich domains in aramid fibers.[1] Based on the morphology,[1,36,37] it is likely that these aggregates are located in the micro- and macrovoids of the aramid fiber as most of the sodium can be solvated in a humid environment and the crystal structure of PPTA leaves no room for the incorporation of sodium salts. They speculated further that some sodium ions could aggregate close to charged end groups in the intercrystalline region.[1,10] They argue that sodium in the voids relates to

DOI: 10.1021/acs.jpcc.9b02071
J. Phys. Chem. C 2019, 123, 14439−14448

sodium sulfate and discuss that sodium ions also coordinate directly to end groups.

This was also expected for our samples based on the sodium/sulfur ratio given in Table 1. However, we observe only one broad heterogeneous sodium distribution for all the different yarns with varying sodium concentrations, including yarns 3 and 4 (0.268 and 0.366%), where a second sodium site can be expected based on the stoichiometry of sodium and sulfur, with excess sodium present compared to sulfate. This excess sodium was expected to coordinate to the carboxylic end groups of the polymer chains (compare Table 1). The fact that we do not observe a second sodium site in the spectra of these yarns means that either the second site is so similar in quadrupolar and chemical shift parameters that the two resonances overlap, even at two vastly different external magnetic fields, or that the sodium ions do not coordinate in large quantities to the carboxylic end groups. That all parameters (linewidth, isotropic chemical shift and quadrupole coupling) of a potential second site are similar to those of the main resonance is, however, very unlikely. Moreover, even when the spectral appearance of the two sites would be similar, their spin−lattice relaxation times (T_1) might differ, but we observe a single T_1 for all samples (see the Supporting Information), including the 0.366% sample (yarn 4), corroborating that sodium occurs in a single pool of sodium ions.

In this discussion, the number of end groups that can be reached by sodium is very important as the end groups are the only groups that do not contain sulfur and are therefore the most probable candidate for a second sodium site. The most plausible explanation for the lack of such a site is that the morphology of the fiber leaves many of the end groups inaccessible to sodium ions as a result of the packing of the molecular chains in the crystallites.

In the fiber morphology models put forward by Morgan et al. and Li et al.,[1,37] the fibers (12 μm in diameter) consist of a skin/core structure, with a skin of the order of 0.1−1 μm. In the skin, the macromolecules are staggered and the end groups are randomly distributed. In the core, rod-like crystallites are oriented along the fiber axis. These crystallites have, according to Morgan et al.,[1] uniform length of approximately 220 nm, whereas the model put forward by Li,[37] based on electron microscopy of dissections of the fiber, allows for different sizes of crystallites. In these crystallites, the end groups are thought to be nonrandomly distributed. It is believed that the end groups and other impurities cluster in the intercrystalline regions where the sodium sulfate and other impurities are located.

For the number of available end groups, the chain length of the macromolecules is also of importance. PPTA is known to have a molecular weight distribution that needs to be accommodated in the morphology models. It is believed that the chain length of individual PPTA molecules is related to the length of the rod-like crystals. The estimate that the chain length is on the order of 100 nm, as estimated for the yarns in this study and by Yang,[38] implies that the end groups are not only clustered in the intercrystalline regions but that, also in the rod-like crystals, staggered packing of the individual PPTA molecules is required to match the observed length of approximately 200 nm for the rod-like crystals in the core of the fiber. A staggered packing of the molecular chains in the rod-like crystallites of the core reduces the availability of the end groups for sodium coordination in the neutralization process and could explain the absence of a second Na site since, in this situation, most carboxylic end groups are not available for coordination to sodium.

Morgan and Pruneda studied impurities in PPTA[10] and speculate that the sodium distribution is more complex than put forward by Table 1. They reason that 80% of the sodium ions are in the form of sodium sulfate, and only a minor fraction of sodium is coordinated to other ionic groups such as sulfonic acid ($-SO_3Na$) or terephthalic acid. This speciation is debated by Yang as it leaves too many acid groups that would degrade the fiber over time.[38] This degradation is, however, not observed for aramid fibers. Furthermore, the presence of sulfuric acid, which is not neutralized in the process, is neglected, and the ratio of sodium/sulfur is not comparable to the values we observed in this study.

If we assume a chain length of individual PPTA molecules around 200 nm or an equivalent of 150−250 repeat units, a value often given in the literature,[1,37,39] a sodium concentration of 0.366 wt % corresponds to eight sodium ions per PPTA macromolecule. In fact, the length of approximately 200 nm in refs 1, 37, and 39 and the references therein are based on the mass average molar mass (M_w). For the average chain length of PPTA, the number average molar mass (M_n) is more representative, and based on the M_n, chain lengths of the order of 100 nm are expected also for the samples described in the cited literature ($M_w \approx 40{,}000$).[1,37,39] For that reason, four sodium ions per macromolecule of PPTA seem more realistic for the 0.366 wt % yarn. Therefore, the main sodium sites are expected to be of sodium sulfate because sulfuric acid is the strongest acid in the system. It is expected that sodium ions aggregate with sulfonic acid groups before coordination to terephthalic acid end groups occurs.

When no coordination to the end groups is present, as the NMR spectra suggest, there is a mismatch in the stoichiometry of sulfur and sodium established by XRF since not all sodium ions will be used up by the formation of sodium sulfate. As we observe that the sodium aggregates are disordered, the incorporation of other ions to counter the charge of sodium upon drying is likely. For instance, immobilized hydroxide ions and water molecules could be present, which introduce disorder in the surroundings of the sodium ions. This may reconcile the mismatch of the sodium/sulfur ratio. A clue toward the presence of residual water molecules is the observation that the linewidth of the sodium resonances is temperature-dependent.

The fact that the sodium ions rapidly (re)hydrate at ambient conditions in all yarns suggests that sodium is present in the intercrystalline region of the fibers. Our study shows that most of these intercrystalline regions are accessible from the exterior of the fibers, allowing water diffusion in and out of the fiber. A previous study shows that, although some impurities can be washed out under harsh conditions, 50% of the impurities remain in the fiber.[10] This is another indication, together with the hydration behavior, that the sodium sulfate resides in the intercrystalline regions in the core of the fiber.

CONCLUSIONS

We have shown that, despite the very low sodium concentration, solid-state NMR can be used for the identification and quantification of the sodium content in aramid fibers. We show that sodium in aramid fibers is not present in the form of well-structured salts but forms disordered aggregates, most likely sodium sulfate hydrates, in

DOI: 10.1021/acs.jpcc.9b02071
J. Phys. Chem. C 2019, 123, 14439−14448

cracks and voids. The ^{23}Na SPE NMR spectra at different magnetic fields can be reasonably described using an extended Czjzek model with an average isotropic chemical shift around −3 ppm and an average quadrupole interaction product of about 2.3 MHz with a distribution parameter σ_Q of 0.4 MHz. Except for the width of the distribution, which is affected by the experimental conditions, the parameters agree well with the line shape observed in an MQMAS experiment. The relatively large quadrupolar coupling, similar to that of crystalline Na_2SO_4, shows that the sodium ions reside in an asymmetric local environment. The large distribution in chemical shift of about 5 ppm indicates substantial structural variation around the sodium ions, particularly considering the fact that ^{23}Na has a small chemical shift range in NMR.

From the invariance of the spectra toward changes in sodium concentration, we infer that the sodium ions are located in ion-rich domains, most likely located in the intercrystalline region of the fiber. The presence of other ions, most probably hydroxides, can give rise to disorder. At ambient conditions, a very large fraction of sodium in polymer systems is hydrated. Therefore, ion pairing of sodium with chemical groups of the polymer chains, as discussed in the literature for different polymers, is very unlikely.

■ ASSOCIATED CONTENT

Supporting Information

The Supporting Information is available free of charge on the ACS Publications website at DOI: 10.1021/acs.jpcc.9b02071.

Field dependence of the second-order quadrupolar interaction, MQMAS spectrum of yarn 3 at 14.1 T, and ^{23}Na spin−lattice relaxation of yarns (PDF)

■ AUTHOR INFORMATION

Corresponding Author

*E-mail: a.kentgens@nmr.ru.nl. Phone: +31 24 36 52078.

ORCID

Arno P. M. Kentgens: 0000-0001-5893-4488

Notes

The authors declare no competing financial interest.

■ ACKNOWLEDGMENTS

The authors thank Teijin Aramid for the supply of the samples. Sander Lambregts and Frank Megens are acknowledged for the initial work in this study as well as Hans Janssen and Gerrit Janssen for the technical support of the experiments. This research is funded by the COAST project 053.21.101. The Netherlands Organization for Scientific Research (NWO) is acknowledged for their financial support of the solid-state NMR facility for advanced material science.

■ REFERENCES

(1) Morgan, R. J.; Pruneda, C. O.; Steele, W. J. The relationship between the physical structure and the microscopic deformation and failure processes of poly(p-phenylene terephthalamide) fibers. *J. Polym. Sci.: Polym. Phys. Ed.* **1983**, *21*, 1757−1783.

(2) Komoroski, R. A.; Mauritz, K. A. A sodium-23 nuclear magnetic resonance study of ionic mobility and contact ion pairing in a perfluorosulfonate ionomer. *J. Am. Chem. Soc.* **1978**, *100*, 7487−7489.

(3) Mauritz, K. A.; Storey, R. F.; Reuschle, D. A.; Beck Tan, N. Poly(styrene-b-isobutylene-b-styrene) block copolymer ionomers (BCPI) and BCPI/silicate nanocomposites. 2. Na+BCPI sol−gel polymerization templates. *Polymer* **2002**, *43*, 5949−5958.

(4) Lim, J. S.; Lee, Y.; Im, S. S. Influence of ionic association on the nonisothermal crystallization kinetics of sodium sulfonate poly(butylene succinate) ionomers. *J. Polym. Sci., Part B: Polym. Phys.* **2008**, *46*, 925−937.

(5) O'Connell, E. M.; Root, T. W.; Cooper, S. L. Morphological studies of lightly-sulfonated polystyrene using ^{23}Na NMR. 1. Effects of sample composition. *Macromolecules* **1994**, *27*, 5803−5810.

(6) O'Connell, E. M.; Root, T. W.; Cooper, S. L. Morphological Studies of Lightly Sulfonated Polystyrene Using ^{23}Na NMR. 2. Effects of Solution Casting. *Macromolecules* **1995**, *28*, 3995−3999.

(7) O'Connell, E. M.; Peiffer, D. G.; Root, T. W.; Cooper, S. L. Morphological Studies of Lightly Sulfonated Polystyrene Using ^{23}Na NMR: Effects of Polydispersity in Molecular Weight. *Macromolecules* **1996**, *29*, 2124−2130.

(8) Connor, C.; Chadwick, M. M. Characterization of absorbed water in aramid fibre by nuclear magnetic resonance. *J. Mater. Sci.* **1996**, *31*, 3871−3877.

(9) Penn, L.; Larsen, F. Physicochemical properties of Kevlar 49 fiber. *J. Appl. Polym. Sci.* **1979**, *23*, 59−73.

(10) Morgan, R. J.; Pruneda, C. O. The characterization of the chemical impurities in Kevlar 49 fibres. *Polymer* **1987**, *28*, 340−346.

(11) Czjzek, G.; Fink, J.; Götz, F.; Schmidt, H.; Coey, J. M. D.; Rebouillat, J.-P.; Liénard, A. Atomic coordination and the distribution of electric field gradients in amorphous solids. *Phys. Rev. B* **1981**, *23*, 2513−2530.

(12) Stöckmann, H.-A. Electric field gradients resulting from randomly distributed unscreened point charges. *J. Magn. Reson. (1969)* **1981**, *44*, 145−158.

(13) Le Caër, G.; Brand, R. A. General models for the distributions of electric field gradients in disordered solids. *J. Phys.: Condens. Matter* **1998**, *10*, 10715.

(14) d'Espinose de Lacaillerie, J.-B.; Fretigny, C.; Massiot, D. MAS NMR spectra of quadrupolar nuclei in disordered solids: The Czjzek model. *J. Magn. Reson.* **2008**, *192*, 244−251.

(15) Le Caer, G.; Bureau, B.; Massiot, D. An extension of the Czjzek model for the distributions of electric field gradients in disordered solids and an application to NMR spectra of 71Ga in chalcogenide glasses. *J. Phys.: Condens. Matter* **2010**, *22*, No. 065402.

(16) Knijn, P. J.; van Bentum, P. J. M.; van Eck, E. R. H.; Fang, C. M.; Grimminck, D. L. A. G.; de Groot, R. A.; Havenith, R. W. A.; Marsman, M.; Meerts, W. L.; de Wijs, G. A.; Kentgens, P. M. A solid-state NMR and DFT study of compositional modulations in AlxGa1-xAs. *Phys. Chem. Chem. Phys.* **2010**, *12*, 11517−11535.

(17) Ahmed, D.; Hongpeng, Z.; Haijuan, K.; Jing, L.; Yu, M.; Muhuo, Y. Microstructural developments of poly (p-phenylene terephthalamide) fibers during heat treatment process: a review. *Mat. Res.* **2014**, *17*, 1180−1200.

(18) Garza, R.; Pruneda, C.; Morgan, R. *Bound water in Kevlar 49 fibers*; 1981; https://www.osti.gov/servlets/purl/6208024.

(19) Mooney, D. A.; MacElroy, J. Differential water sorption studies on Kevlar™ 49 and as-polymerised poly (p-phenylene terephthalamide): adsorption and desorption isotherms. *Chem. Eng. Sci.* **2004**, *59*, 2159−2170.

(20) Vijayan, K. X-ray evidence for the presence of single crystals of sodium salts in Kevlar 49 fibres. *Curr. Sci.* **1987**, *56*, 1055−1056.

(21) Pauw, B. R.; Ohnuma, M.; Sakurai, K.; Klop, E. A. 2D anisotropic scattering pattern fitting using a novel Monte Carlo method: Initial results. *arXiv:1303.2903 [physics]* **2013**, arXiv: 1303.2903.

(22) Zhu, C.; Liu, X.; Guo, J.; Zhao, N.; Li, C.; Wang, J.; Liu, J.; Xu, J. Relationship between performance and microvoids of aramid fibers revealed by two-dimensional small-angle X-ray scattering. *J. Appl. Cryst.* **2013**, *46*, 1178−1186.

(23) Fenzke, D.; Freude, D.; Fröhlich, T.; Haase, J. NMR intensity measurements of half-integer quadrupole nuclei. *Chem. Phys. Lett.* **1984**, *111*, 171−175.

(24) Kentgens, A. P. M. A practical guide to solid-state NMR of half-integer quadrupolar nuclei with some applications to disordered systems. *Geoderma* **1997**, *80*, 271−306.

DOI: 10.1021/acs.jpcc.9b02071
J. Phys. Chem. C 2019, 123, 14439−14448

(25) Turoscy, R.; Leidheiser, H., Jr.; Roberts, J. E. Solid-State NMR Studies of Sodium Ions in a Polybutadiene Matrix. *J. Electrochem. Soc.* **1990**, *137*, 1785−1788.
(26) Wang, P.; Ando, I. Structural characterization of hydrated poly(aspartic acid) sodium and poly(aspartic acid) sodium/poly(vinyl alcohol) blends by high-resolution solid-state ^{23}Na NMR. *J. Mol. Struct.* **1999**, *508*, 97−102.
(27) Mauritz, K. A.; Moore, R. B. State of Understanding of Nafion. *Chem. Rev.* **2004**, *104*, 4535−4586.
(28) Turoscy, R.; Leidheiser, H.; Roberts, J. E. Solid-State NMR Studies of Ions in Protective Coatings II. Lithium and Cesium Ions in Polybutadiene Coatings. *J. Electrochem. Soc.* **1992**, *139*, 779−783.
(29) Medek, A.; Harwood, J. S.; Frydman, L. Multiple-quantum magic-angle spinning NMR: A new method for the study of quadrupolar nuclei in solids. *J. Am. Chem. Soc.* **1995**, *117*, 12779−12787.
(30) Frydman, L.; Harwood, J. S. Isotropic spectra of half-integer quadrupolar spins from bidimensional magic-angle-spinning NMR. *J. Am. Chem. Soc.* **1995**, *117*, 5367−5368.
(31) van Meerten, S. G. J.; Franssen, W. M. J.; Kentgens, A. P. M. ssNake: A cross-platform open-source NMR data processing and fitting application. *J. Magn. Reson.* **2019**, 56−66.
(32) Engelhardt, G.; Kentgens, A. P. M.; Koller, H.; Samoson, A. Strategies for extracting NMR parameters from ^{23}Na MAS, DOR and MQMAS spectra. A case study for $Na_4P_2O_7$. *Solid State Nucl. Magn. Reson.* **1999**, *15*, 171−180.
(33) Sato, R. K.; McMillan, P. F.; Dennison, P.; Dupree, R. High-resolution aluminum-27 and silicon-29 MAS NMR investigation of silica-alumina glasses. *J. Phys. Chem* **1991**, *95*, 4483−4489.
(34) Dickinson, L. C.; MacKnight, W. J.; Connolly, J. M.; Chien, J. C. W. ^{23}Na-NMR of solid state ionomers: lineshape, shift, and hydration effects. *Polym. Bull.* **1987**, *17*, 459−464.
(35) Dec, S. F.; Maciel, G. E.; Fitzgerald, J. J. Solid-state sodium-23 and aluminum-27 MAS NMR study of the dehydration of sodium aluminate hydrate ($Na_2O{\cdot}Al_2O_3{\cdot}3H_2O$). *J. Am. Chem. Soc.* **1990**, *112*, 9069−9077.
(36) Dobb, M. G.; Johnson, D. J.; Majeed, A.; Saville, B. P. Microvoids in aramid-type fibrous polymers. *Polymer* **1979**, *20*, 1284−1288.
(37) Li, L. S.; Allard, L. F.; Bigelow, W. C. On the morphology of aromatic polyamide fibers (Kevlar, Kevlar-49, and PRD-49). *J. Macromol. Sci., Part B: Phys.* **1983**, *22*, 269−290.
(38) Yang, H. H. *Kevlar Aramid Fiber*; John Wiley & Sons, Ltd: 1993.
(39) Li, S. F. Y.; McGhie, A. J.; Tang, S. L. Internal structure of Kevlar® fibres by atomic force microscopy. *Polymer* **1993**, *34*, 4573−4575.

DOI: 10.1021/acs.jpcc.9b02071
J. Phys. Chem. C 2019, 123, 14439−14448